

Surface deposits and landslide inventory map of the area affected by the 1997 Umbria-Marche earthquakes

GUENDALINA ANTONINI (*), FRANCESCA ARDIZZONE (**), MAURO CARDINALI (**), MIRCO GALLI (*), FAUSTO GUZZETTI (**), & PAOLA REICHENBACH (**)

ABSTRACT

On 26 September 1997 the Umbria-Marche area of Central Italy was shaken by two severe earthquakes of 5.6 and 5.8 local magnitude. On 14 October 1997 the same area experienced another earthquake of similar magnitude. Following the main shocks we performed field surveys to map landslides triggered by the earthquakes, and to determine the main landslide types, and whether there was a relationship between pre-existing landslide deposits and the seismically induced failures. Information collected at 220 sites revealed that most of the fractures were related to the presence of human structures, and that landslides were mostly rock falls, minor rock-slides and topples. We mapped new fractures in a few pre-existing landslide deposits, but no major landslide was reactivated to the point of catastrophic failure. For an area of about 900 km² located around the earthquake epicentres, standard photo-geological techniques and field surveys enabled us to prepare a detailed map of surface deposits, showing landslides, alluvial fans and other types of debris. A geographical database including all the available information was prepared to investigate the relationship between co-seismic landslides and fractures and the distribution of surface deposits, including landslides.

KEY WORDS: *Landslide, Debris, Surface deposit, Map, Earthquake, Umbria-Marche Apennines, Italy.*

RIASSUNTO

Carta dei depositi superficiali ed inventario dei movimenti franosi nell'area colpita dal terremoto Umbro-Marchigiano del 1997.

Il 26 settembre 1997 l'Appennino Umbro-Marchigiano fu colpito da due terremoti di magnitudo locale pari a 5.6 e 5.8. Il 14 ottobre dello stesso anno la stessa area fu colpita da un altro evento sismico di magnitudo locale simile ($M_L=5.5$). Le scosse principali furono seguite da numerosissime repliche, alcune delle quali anche particolarmente intense. A seguito delle scosse principali abbiamo effettuato numerosi sopralluoghi sul terreno allo scopo di identificare e cartografare i movimenti franosi causati dalle scosse sismiche, per individuare le tipologie di frane più frequenti, e per identificare le possibili relazioni fra la distribuzione delle frane preesistenti e quelle indotte dalla sequenza sismica. Gli effetti al suolo osservati possono essere raggruppati in: fratture del suolo, movimenti franosi, fenomeni di compattazione, fagliazioni superficiali, e variazioni nel regime e nella qualità delle sorgenti. Questo lavoro descrive unicamente le prime due tipologie d'effetti al suolo, ossia le fratture del suolo ed i movimenti franosi. Le informazioni raccolte in oltre 220 località da noi visitate hanno evidenziato come la maggior parte delle fratture fosse correlata alla presenza di manufatti (strade, case, rilevati, ponti, una diga) e che i movimenti franosi più frequenti siano stati le cadute di massi, i ribaltamenti e le frane in roccia di piccole o modeste dimensioni. Abbiamo osservato fratture d'origine sismica all'interno ed ai bordi di corpi di frana preesisten-

ti, ma nessuna frana è stata riattivata fino al collasso. Per un'area di circa 900 km² attorno all'area epicentrale, attraverso l'utilizzo sistematico di tecniche foto-geologiche e rilevamenti di campagna abbiamo realizzato una dettagliata carta dei depositi superficiali. La mappa, realizzata a scala 1:10.000, riporta la localizzazione dei movimenti franosi, delle conoidi alluvionali, e di altri tipi di detrito. Per studiare le relazioni fra le frane e le fratture sismoindotte e la distribuzione dei depositi superficiali (incluse le frane preesistenti), abbiamo realizzato un archivio geografico. L'archivio ha permesso fra l'altro di studiare l'abbondanza e la distanza dei dissesti dagli ipocentri delle scosse principali.

TERMINI CHIAVE: *Frane, detrito, depositi superficiali, cartografia, terremoto, Appennino umbro-marchigiano, Italia.*

INTRODUCTION

Earthquake tremors began in the Regions of Umbria and Marche in central Italy on 3 September 1997. On 26 September at 2:33 a.m. (0.33 GMT) the area was shaken by a severe earthquake of local magnitude $M_L=5.6$ ($M_S=5.5$). The epicentre was located to the south of the village of Colfiorito. A few hours later, at 11:40 a.m. (9:40 GMT), another earthquake of slightly larger magnitude ($M_L=5.8$, $M_S=5.9$) shook the same area. Vertical accelerations of more than 0.4 g were recorded. The hypocentres of both earthquakes were located at a depth of about 12 kilometres. During the earthquake sequence that began in September 1997 and lasted for several months hundreds of aftershocks occurred in an area bounded to the north by the town of Gualdo Tadino and to the south by Norcia (fig. 1). At 1:24 a.m. local time on 7 October, an $M_L=5.3$ earthquake was recorded to the west of the first shock with a hypocentral depth of about 14 kilometres. On 14 October, at 17:23 a.m. (15:23 GMT), the Umbria-Marche Apennines were shaken by an earthquake of similar magnitude ($M_L=5.5$, $M_S=5.5$), with an epicentre located near the village of Forfi. Lastly, on 3 April 1998 an earthquake of local magnitude 5.0 was recorded between Gualdo Tadino and Nocera Umbra (fig. 1) (BOSCHI *et alii*, 1998; SERVIZIO SISMICO NAZIONALE & ENEL, 1998).

This sequence of earthquakes killed ten people, left thousands homeless, and caused extensive damage to the towns and villages of the area. Damage to the cultural heritage was extremely large: tens of churches and historical buildings (including the upper basilica of San Francisco in Assisi) were severely damaged. The main shocks and the several hundreds of perceptible aftershocks caused numerous ground fractures and landslides, most of which were rock-falls and topples. These caused problems for roads and other components of the regional infrastructure.

(*) Terra s.n.c., Perugia, Italy.

(**) CNR-IRPI, Via della Madonna Alta, 126 - 06128 Perugia, Italy
- email: M. Cardinali@irpi.pg.cnr.it

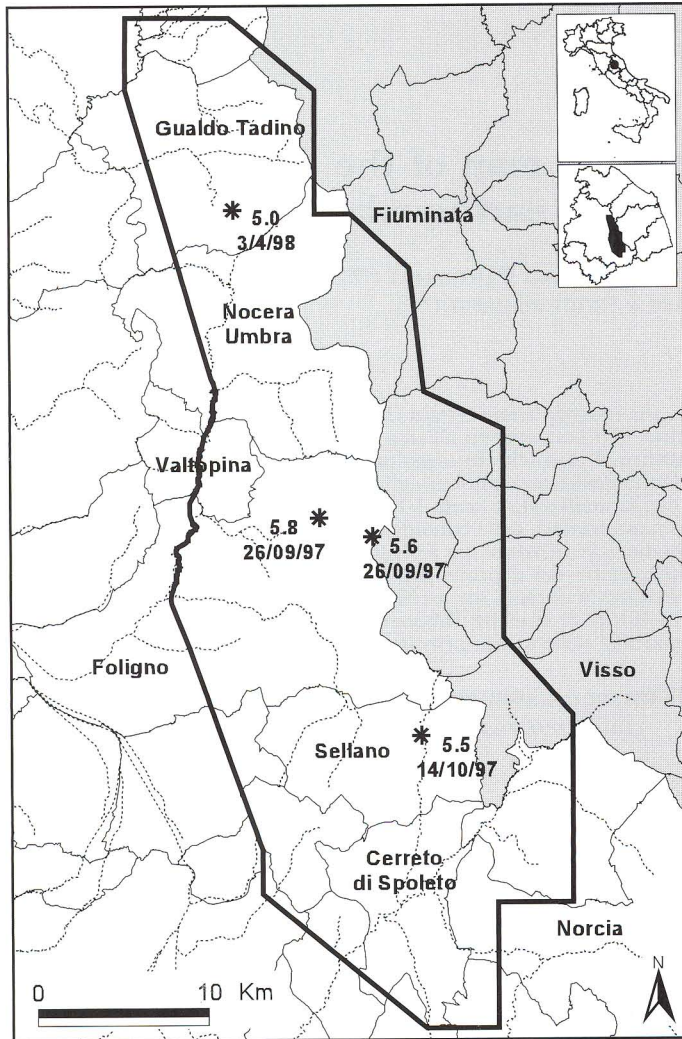


Fig. 1 - Location of the study area. The location of the earthquake epicentres is shown, together with the extent of the area covered by the surface deposits and landslide inventory map. For each epicentre the date and the local magnitude are given. Municipality boundaries (thin lines) and major rivers (dotted lines) are shown for location purposes. Dark grey: Marche Region. White: Umbria Region.
 - Localizzazione dell'area di studio. È indicata la localizzazione degli epicentri delle scosse principali, assieme all'estensione dell'area coperta dalla carta inventario dei movimenti franosi e dei depositi superficiali. Per ciascun epicentro sono indicate la data e la magnitudo locale. Sono anche indicati i limiti comunali (linee sottili) ed i fiumi principali (linee tratteggiate). Grigio scuro: Regione Marche. Bianco: Regione Umbria.

The area affected by the 1997 seismic sequence and the surrounding territories of the Umbria Marche Apennines have a long history of earthquakes. BOSCHI *et alii* (1998) reported 35 earthquakes in the Umbria-Marche area with a magnitude greater than 4.5 between 99 b.C. and 1984. Maximum earthquake intensity ranged from 6 to 11 MCS, and magnitude ranged from 4.7 to 6.7. Some of the historical earthquakes are known to have triggered landslides. The oldest reported seismically induced landslide in the area is probably a rockslide at Serravalle del Chienti triggered by the 30 April 1279 earthquake. The earthquake had an estimated magnitude of 6.3 and its epicentre was located between Serravalle del Chienti and Nocera Umbra. The slide involved a volume of about one

million cubic meters of rock and occurred few hundred meters to the north of the Serravalle Castle (BOSCHI *et alii*, 1998 pp. 36-38). The earthquake of 5 January 1838 in Valnerina (Magnitude=5.3, Intensity=8) triggered rock-falls at Borgiano, at Grutti (where a rockfall destroyed a house), and along the Nera valley between Borgo Cerreto and Biselli (the same area affected by numerous rockfalls triggered by the 1997 earthquakes). Few years later, the 22 August 1859 earthquake in Valnerina (Magnitude=5.8, Intensity=9) triggered rock-falls at M. Pattino (near Norcia) (SGA, 1990). ESPOSITO *et alii* (2000) described other earthquake-induced landslides in central Apennines.

The paper reports the results of a research effort that started a few days after the first earthquakes aimed at: mapping the distribution of pre-existing landslides and surface deposits; studying the type and pattern of ground effects triggered by seismic shaking; and investigating the relationships between the co-seismic ground effects and the distribution of pre-existing landslides and surface deposits.

SURFACE DEPOSITS AND LANDSLIDE INVENTORY MAP

Starting immediately after the earthquakes of 26 September, we carried out field surveys to determine where landslides had been triggered by the earthquakes, what the main landslide types were, and whether a relation could be discerned between pre-existing landslide deposits and new, seismically-induced failures. Working in small teams, we compiled 1:10,000-scale maps and took photographs of the location of fractures and landslides. Most of the 220 sites that we visited were situated along roads. Due to time constraints and resource limitations, we were able to record only a restricted amount of information at each site.

Besides mapping the earthquake's ground effects in the field, for an area of 900 km² around the epicentral area (bounded by $M_L > 4.0$), we prepared a map of landslides and other surface deposits. The study area extends from Fossato di Vico in the north to Cerreto di Spoleto in the south, and from Valtopina in the west to the Chienti Valley and the upper Valnerina Valley in the east (fig. 1). The map was prepared using photo-geological techniques (RAY, 1960; MILLER, 1961; ALLUM, 1966; AMADESI, 1977; VAN ZUIDAN, 1985) and reconnaissance field surveys. Interpretation was based upon 1:13,000-scale, black-and-white, vertical aerial photographs taken in October and November 1997. Very large-scale (1:2000) aerial photography taken immediately after the 26 September earthquakes was available around towns and villages, and we used it to refine the interpretation. For comparison purposes, and in order to identify and map large landslides better, we also used 1:33,000-scale, black-and-white aerial photographs taken in 1954-5.

Interpretation of aerial photographs was carried out by a team of three geomorphologists over a four month period, from January to April 1998. Two team members looked at each pair of aerial photographs using a stereoscope that allowed both interpreters to map contemporaneously on the same stereo pair. The third photo-interpreter independently reviewed, and where necessary corrected, the interpretations of the other two. This approach was time consuming, but guaranteed the consistency of the photo-geological map. For the purposes of

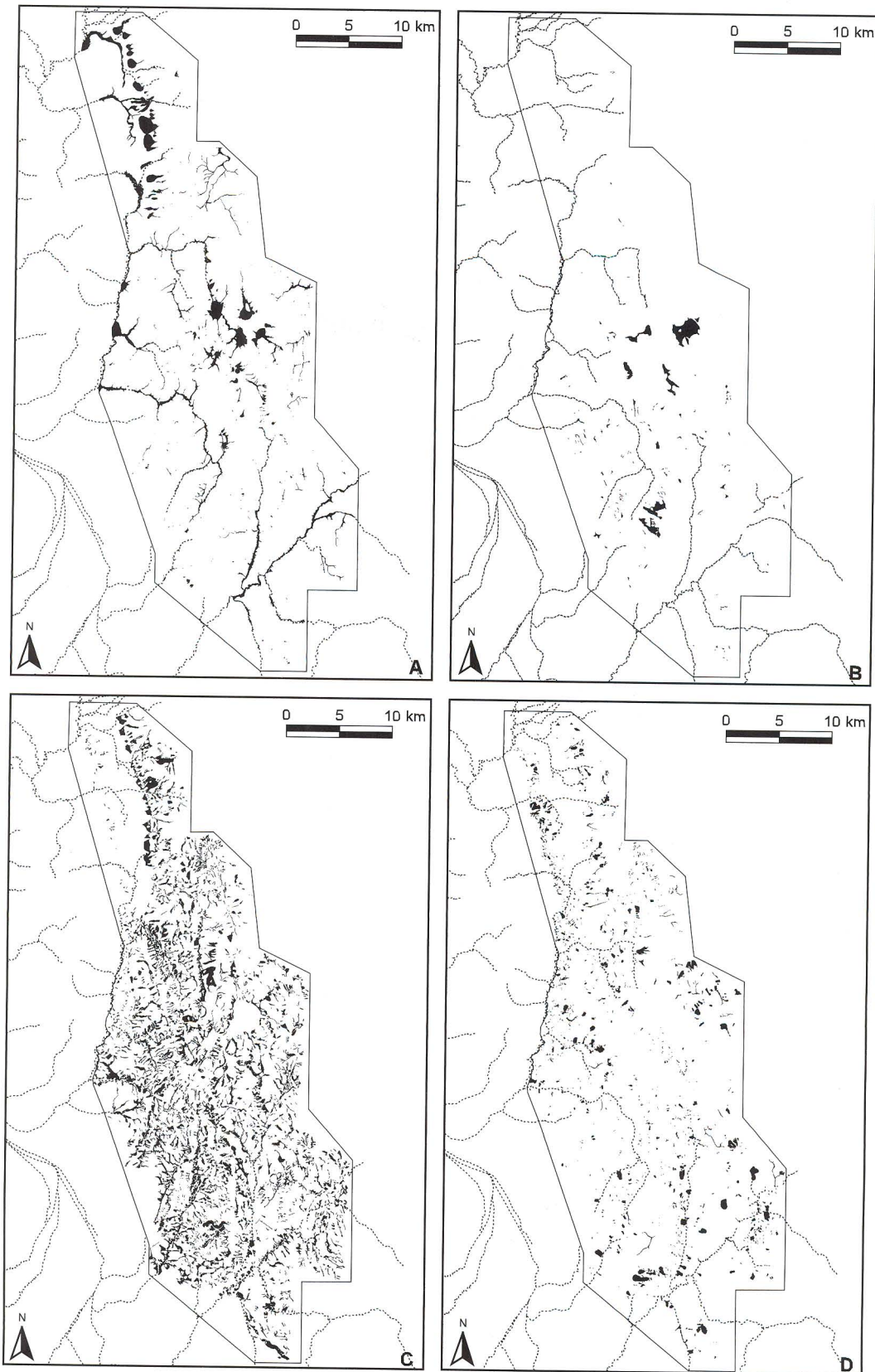


Fig. 2 - Maps showing the pattern and extent of landslides and surface deposits. Original map at 1:10,000 scale. A) map of alluvial sediments, covering 66.8 km² of the study area. B) map of deposits in closed depressions, covering about 12 km² of the study area. C) map of debris deposits (including debris flows), covering 33.3 km² of the study area. D) map of landslide deposits (including debris flows), covering 128.3 km² of the study area.

- Carta inventario dei movimenti franosi e dei depositi superficiali. Scala originale 1:10.000. A) carta dei depositi alluvionali che coprono 66,8 km² dell'area. B) carta dei depositi nelle depressioni chiuse, che coprono 12 km² dell'area. C) carta dei depositi di detrito, inclusi i depositi eluviali e colluviali, i talus ed i coni di detrito, che coprono 128,3 km² dell'area. D) carta dei depositi di frana (comprese le colate di detrito), che coprono 33,3 km² dell'area.

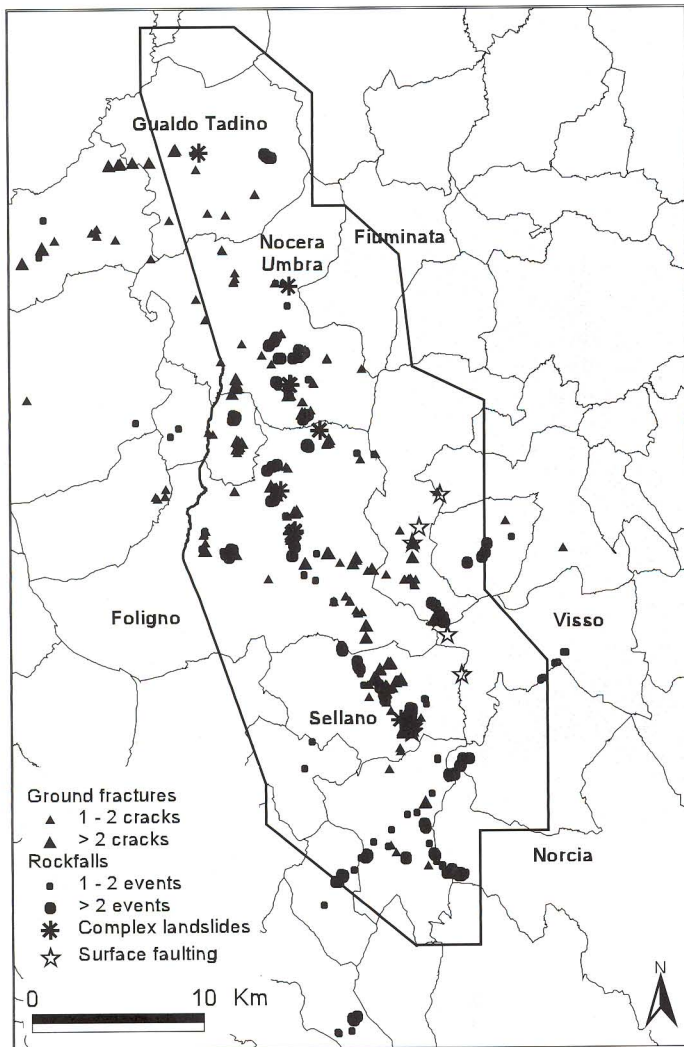


Fig. 3 - Map showing the distribution of the ground effects induced by the Umbria-Marche 1997 earthquake sequence. Ground effects were observed at more than 220 sites. They include: ground fractures (triangles); rockfalls, including topples and minor rockslides (dots); complex landslides (asterisks); and surface faultings (stars). - *Carta della distribuzione degli effetti al suolo prodotti dalla sequenza sismica del 1997. Gli effetti al suolo sono stati rilevati in oltre 220 località e comprendono: fratture del suolo (triangoli); cadute di massi, compresi i ribaltamenti e le frane in roccia minori (punti); frane complesse (asterischi), ed alcune fagliamenti superficiali (stelle).*

interpretation, we used all geological and geomorphological information available to us from published maps, previous works carried out in the same area, and discussion with other geologists. A few field surveys were carried out to test the reliability of the photo-geological map and to solve local interpretation problems.

Information obtained in the field and through the interpretation of aerial photographs was transferred to 1:10,000 scale orthophoto maps, published in 1981-3 by the Umbria Regional Government. These were the only large-scale maps available for the entire study area. A total of 36 sheets were used to cover a mostly mountainous territory of about 900 km². The quality of the orthophoto maps is inferior to that of topographical maps at the same scale, and the reliability of the elevation data in the orthophoto maps is locally poor, as contour lines fail

to capture the complexity of the terrain at the local level. However, orthophoto maps allowed us to sketch geomorphological features such as landslides, alluvial fans and escarpments directly onto rectified, vertical photographs of the ground, which helped to determine the precise location of ground fractures. Unfortunately, due to locally large differences between the orthophoto maps and other topographical maps at the same or smaller scales (Regional Technical Maps or 1:25,000 national quadrangles), it was not a straightforward matter to automatically superimpose geographical information obtained from different maps by digitisation.

We transferred geomorphological information from the orthophoto maps onto stable, transparent sheets and scanned these to obtain black and white, raster images of each map sheet. We used a scanning resolution of 300-400 dpi, which corresponded to a ground resolution of 0.1 m or less. The raster representation of the geomorphological line images was then changed into vector format using a semi-automatic procedure, which allowed us to assign attributes to each line segment. Polygons were then constructed and labelled with the appropriate codes, depending on their geological and geomorphological properties. Lastly, map sheets were collected together in a geographical database, and colour plots were prepared to test the digitisation procedure.

PHOTO-GEOLOGICAL CRITERIA

Recognition of geomorphological features from stereoscopic aerial photographs is a complex, largely empirical technique that requires experience, training, a systematic methodology and well-defined interpretation criteria (VAN ZUIDAN, 1985). The photo-interpreter classifies geological objects and morphological forms based on his or her experience, and on the analysis of a set of characteristics which can be identified on photographic images. These include shape, size, photographic colour, tone, mottling, texture, pattern of objects, site topography and setting (RAY, 1960; MILLER, 1961; ALLUM, 1966; RIB & LIANG, 1978; VAN ZUIDAN, 1985). Shape refers to the form of the topographic surface. Because of the vertical exaggeration of stereoscopic vision, shape is the single most useful characteristic for the classification of an object from aerial photographs. Size describes the areal extent of an object. Knowing the physical dimensions of an object is seldom enough for classification, but it can be very useful to identify properties such as extent and depth. Colour, tone, mottling and texture depend on the light reflected by the surface, and can be used to infer rock, soil and vegetation types, the latter being a proxy for wetness. Mottling and texture are measures of terrain roughness and can be used to identify surface types and the size of debris. Pattern is the spatial arrangement of objects in a repeated or characteristic order or form, and is used to infer rock type and resistance to erosion, as well as the presence of faults and other tectonic lineaments. Topographic site is the position of a place with reference to its surroundings. It reflects morphometric characters such as height difference, slope steepness and aspect, and the presence of convexities or concavities in the terrain. Setting expresses regional and local characteristics (lithological, geological, morphological, climatic, vegetational, and so on) in relation to the surroundings. Site topography and setting are particularly suited to



Fig. 4 - Vio. Example of seismically induced ground fractures opened along a road.
- Vio. Esempio di fratture al suolo sismoindotte apertesi lungo una strada.

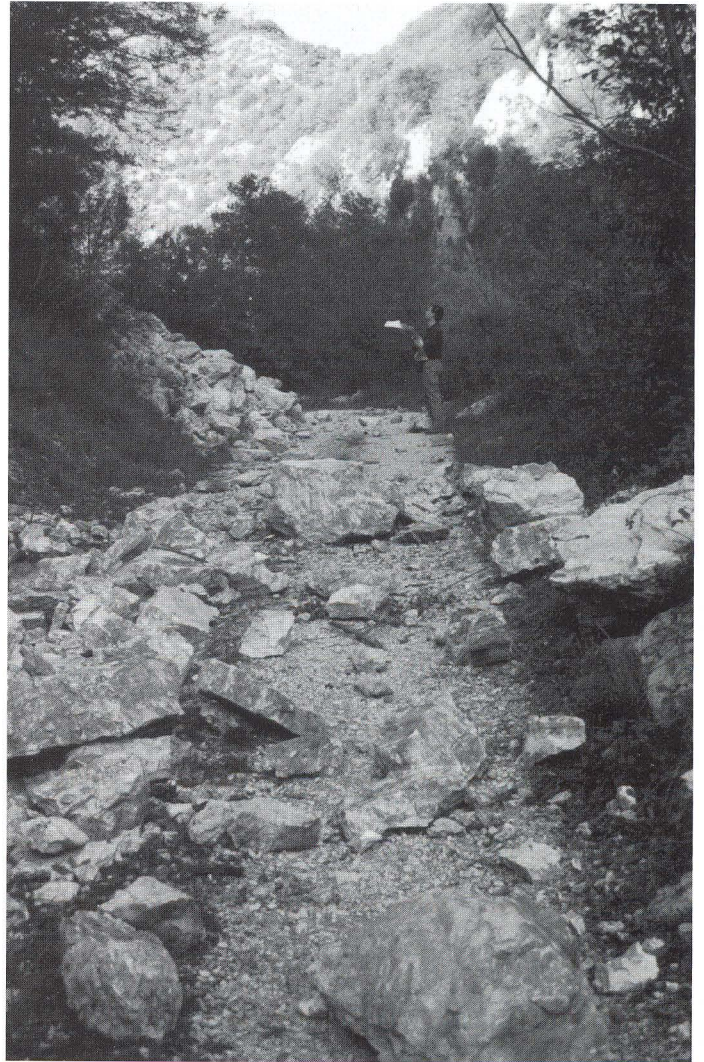


Fig. 5 - Vigi Valley, near Sellano. Examples of earthquake induced rockfalls along a road. The 14 October 1997 earthquake triggered these landslides.
- Valle del Vigi nei pressi di Sellano. Esempio di cadute di massi prodotte dal terremoto del 14 ottobre 1997 lungo una strada.

inferring rock type and structure, attitude of bedding planes, and presence of faults and other tectonic features (RAY, 1960; MILLER, 1961; ALLUM, 1966; AMADESI, 1977; VAN ZUIDAN, 1985).

By employing the relationship between a form and a geological or geomorphological feature, morphological correlation is used to classify an object on the basis of photographic interpretation. For example, an upper concavity and lower convexity on a slope typically indicates the presence of a landslide. Furthermore, the combination of cone-shaped geometry (in plan) and upwardly convex slope profile is diagnostic of an alluvial fan or debris cone. In addition, a closed depression in limestone terrain (i.e., a sinkhole) may harbour residual deposits, while a gentle slope at the foot of a steep, rocky cliff is usually a talus deposit. Great care must be taken when inferring the characteristics and properties of geological and geomorphological objects from aerial photographs because morphological convergence is possible. For instance, in glacial terrain landslide and moraine deposits may appear similar; and in steep terrain a deep-seated

gravitational deformation may look like a tectonic structure.

All the previously described interpretation criteria were used in preparing the surface deposits and landslide inventory map. It was simpler to recognize and map landslides than to identify and depict other surface deposits. Mass-transport deposits (e.g., deep seated landslides) exhibited a distinct, easily recognisable morphology with sharp boundaries. Limits were easily identified for talus deposits and for the apex of alluvial fans and debris cones. However, they were less distinct for shallow landslides and for alluvial deposits and were part of a continuum for the residual surface cover and the distal ends of the largest alluvial fans.

LEGEND

To prepare a photo-geological map a legend is needed. This must meet the project goals, must be capable of portraying important (or even subtle) geological and geomorphological characteristics, and must be compatible



Fig. 6 - Corno Valley, near Triponzo. Examples of an earthquake induced rockslide along a dismissed road. The 14 October 1997 earthquake triggered the landslide.

- Valle del Corno nei pressi di Triponzo. Esempio di frana in roccia prodotta dal terremoto del 14 ottobre 1997 lungo una strada dismessa.



Fig. 7 - Stravignano. Examples of an earthquake-induced rock topple along a road. The travertine cap failed during the night of 16-17 October 1997, and was the result of the cumulative effect of ground shaking produced by several aftershocks.

- Stravignano. Esempio di ribaltamento lungo una strada. La piastra di travertino cedette nella notte fra il 16 ed il 17 ottobre 1997 a causa dell'effetto cumulato di numerose scosse.

with the technique used to capture the information (i.e., with the scale, type and vintage of aerial photographs, the scale of the map, the type of stereoscope, the availability of geological data, the complexity of the terrain, and the time and resources available). Ideally the legend should be prepared (and agreed upon) by its users before interpretation begins. In reality, the legend tends to be changed during a photo-interpretation project. Classes are added, deleted, split or merged to conform with local geological and geomorphological settings, the interpreter's experience and preferences, and new findings.

One of the goals of our project was to map landslides and surface deposits, and to distinguish them on the map from outcrops of bedrock (fig. 2). Hence, we gave the legend three sections: for landslides, surface deposits and bedrock. An attempt was made to estimate a degree of certainty in the recognition of all mapped features. Landslides and debris deposits that were clearly recognised were classified as certain. Deposits for which the identification was difficult, the boundary undetermined or the position tentative were classified as uncertain. Since some of the deposits were easier to recognise and map than others, the degree of certainty varied throughout the map.

Landslides

Using a methodology already tested in the Umbria-Marche area (GUZZETTI & CARDINALI, 1989; ANTONINI *et alii*, 1993) landslides were mapped on the basis of their type, estimated degree of activity, depth of movement and velocity. The last of these was inferred in relation to the type of movement.

Slow mass movements include slides, slide-earth flows and flows. No distinction was made between these three types of landslides. The degree of activity was tentatively estimated for two classes (active and inactive) based on morphological appearance: i.e., the «freshness» of the landslide as it appeared on aerial photographs. Depth (shallow, ≤ 5 m, vs. deep-seated, > 5 m) was estimated on the basis of landslide type and size. For deep-seated landslides the scarp area was mapped separately from the landslide deposit. This distinction was not made for shallow landslides.

Fast moving landslides include rockfalls, rockslides, topples and debris flows. In general, the size of these failures, which varied from <1 m³ to a few tens of cubic metres did not permit them to be recognized on aerial photographs. Rockfalls, rockslides and topples were mapped through reconnaissance surveys in the field or during site-specific investigations designed to ascertain landslide risk for civil protection purposes. Bedrock escarpments ranging from a few tens of metres to about a hundred metres high were identified from aerial photographs and their upper edges were mapped as possible sources of failures. Rockfall and rockslide deposits were found to be abundant on talus and debris cones. Occasionally, boulders were large enough to be seen on aerial photographs.

The source and deposition areas of debris flows were mapped separately using aerial photographs. Source areas were small and were generally mapped as points at the 1:10,000 scale. They were found to be located on the upper parts of slopes, where hollows or depressions were present and soil or loose debris were abundant. Some of the source areas appeared to show the headscarps of eroding rills. Debris flow deposits were observed on

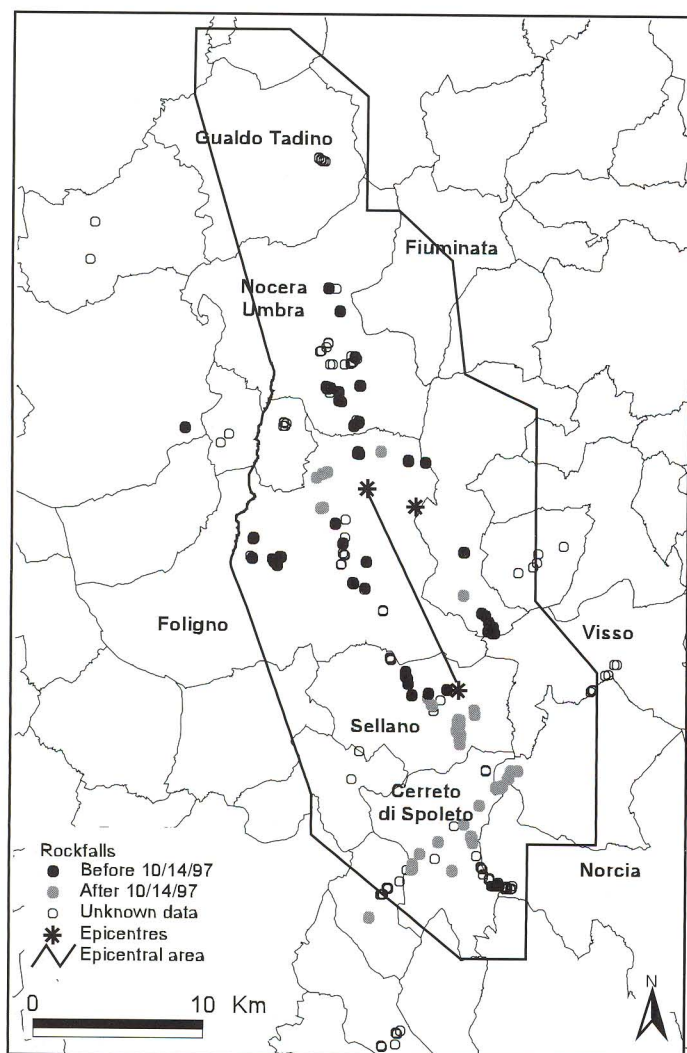


Fig. 8 - Map showing rockfalls (including topples and minor rockslides) triggered by the 1997 earthquake sequence in the Umbria-Marche area. See also fig. 9.

- Carta delle distribuzione delle cadute di massi (inclusi i ribaltamenti e le frane in roccia) innescate dalla sequenza sismica del 1997 nell'area umbro-marchigiana. Vedere anche la fig. 9.

debris cones, talus deposits, alluvial fans and along some of the tributary valleys. The extent and volume of the deposits varied substantially. On talus and debris cones, debris flow deposits were small, were located at the mouths of steep channels, and exhibited a distinct conical shape. The boundaries with neighbouring deposits or with the bedrock were sharp and easily recognisable. Debris flow deposits on alluvial fans and along the tributary valleys were larger in size and exhibited a more subdued morphology, with gradational boundaries separating them from neighbouring deposits.

Surface deposits

Surface deposits included alluvial sediments, deposits in closed depressions, and debris deposits. The first of these included fluvial sediments and alluvial fans. Fluvial fills of recent to current age were found to be abundant on the valley floor of both perennial and seasonal rivers. The latter were present along the tributaries of larger rivers. Fluvial sediments were recognised on the basis of

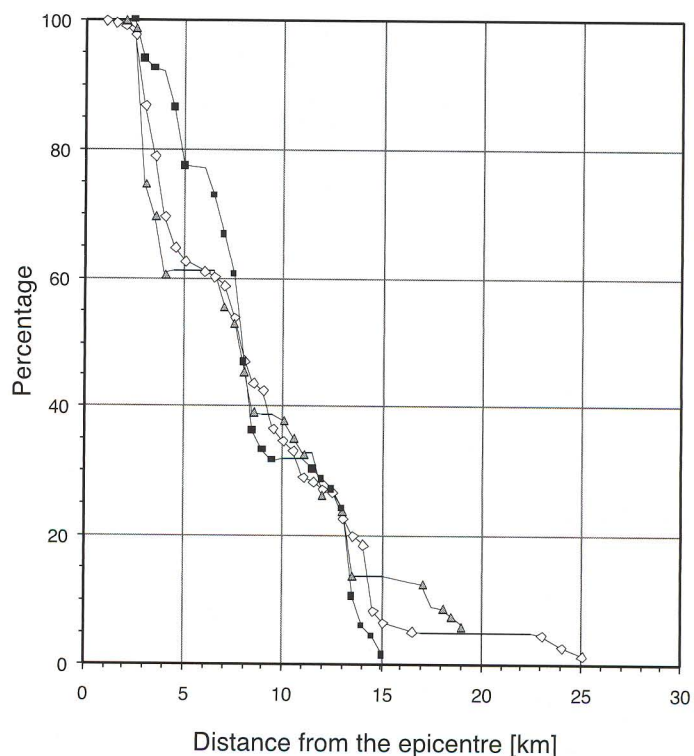


Fig. 9 - Distance to the epicentres of the observed rockfalls (including topples and minor rockslides). Black squares: data-set A, 33 rock-fall sites triggered by the 26 September earthquakes and its aftershocks. Grey triangles: data-set B, 32 rock-fall sites triggered by the 14 October earthquake and its aftershocks. Open diamonds: data-set C: a «cumulative» data-set with all recorded rock-falls, including those for which the date of occurrence is unknown or uncertain. For data-set C the distance was computed to the epicentral area, defined as the line joining the 26 September and the 14 October earthquakes.

- Distanza delle cadute di massi osservate (inclusi i ribaltamenti e le frane in roccia minori) dagli epicentri. Quadrati neri: gruppo A, 33 siti con cadute massi innescate dal terremoto del 26 settembre. Triangoli grigi: gruppo B, 32 siti con cadute massi innescate dal terremoto del 14 ottobre. Rombi aperti: gruppo C, tutte le cadute massi osservate, indipendentemente dalla data di occorrenza. Sono inclusi eventi di cui non è nota la data. Per il gruppo C la distanza è stata calcolata rispetto all'area epicentrale, definita dalla linea che unisce gli epicentri del 26 settembre e del 14 ottobre 1997.

their position and morphological setting. On aerial photographs they appeared to be dark to light in tone, with a fine texture and a flat surface. Terraced fluvial sediments, small ponds, swamps and areas prone to inundation were mapped locally.

Alluvial fans were located along the main valleys, at the mouth of rivers and gullies, and within inter-mountain basins (e.g. at Piani di Colfiorito). Alluvial fans showed an easily recognisable conical shape with convex-upward longitudinal and transverse profiles. They were recognised on the basis of their shapes and positions; on aerial photographs they exhibited light grey tones and a rough texture, indicating the presence of coarse sediments. Small fans were mostly covered by trees or shrubs, whereas the largest fans were cultivated, particularly in the inter-mountain basins. For the latter, the pattern of land use tended to show the extent of the fans.

Although no quantitative dating was performed, fans of different ages were recognised in the area. This was clear in the Gualdo Tadino basin where at least three gen-

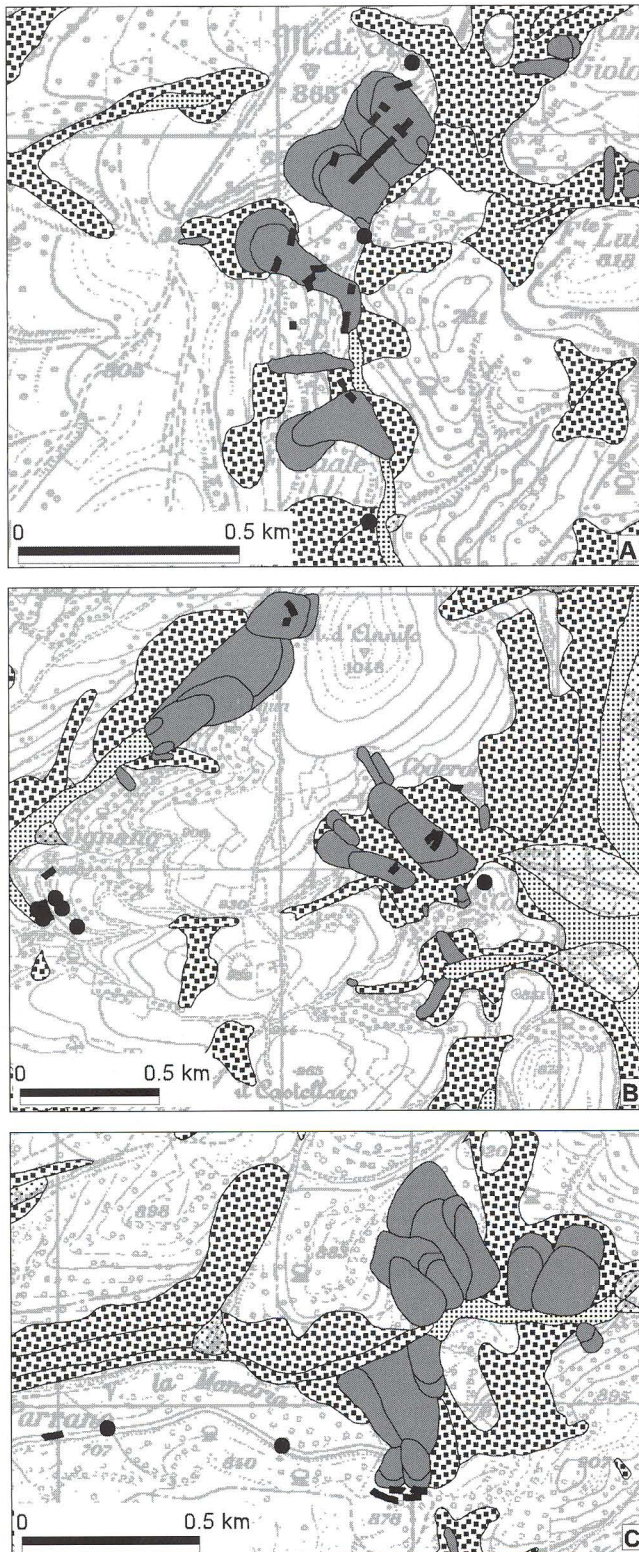


Fig. 10 - Maps showing the relationship between the pre-existing landslides (dark grey), surface deposits (various dotted patterns) and the location of fractures (thick lines) and rock-falls (dots). A) The Franca landslide, along a right tributary of the Menotre River, to the East of Foligno. B) The Annifo and Monte Annifo landslides. C) The Pian dell'Aia landslide, along the La Mandria Valley north of Nocera Umbra. - Carte illustranti le relazioni fra le frane pre-esistenti (grigio scuro), i depositi superficiali (vari pattern) e la localizzazione delle fratture (linee spesse) e delle cadute massi (punti). A) Frane di Franca, lungo un affluente di destra del Fiume Menotre, ad est di Foligno. B) Frane di Annifo e di Monte Annifo. C) La frana di Pian dell'Aia, lungo il torrente La Mandria, a nord di Nocera Umbra.

erations of deposits were identified, namely recent fans located at the outlet of all of the gullies draining the western slopes of the Monte Maggio-Monte Penna ridge; dissected fans present on top of the recent fans at the outlets of some of the largest valleys (i.e., in the Fonno, Feggia, Cannuie and Fosso della Vena valleys); and distal fans making up a continuous bajada covering most of the Gualdo Tadino basin. The sediments of the last of these are only a few metres thick and are limited in the west by the fluvial deposits of the River Rasina.

Deposits in closed depressions included residual sediments in sinkholes and uvalas (e.g., at Pupaggi, Fonni, Mt. Cammoro, Collattoni, and Mt. Aguzzo); and lake, pond and swamp sediments deposited in low-energy environments during the filling up of topographic lows of tectonic origin (e.g., at Piani di Colfiorito). The deposits were recognised and classified on the basis of their position within karstic or tectonic depressions and their topographic settings (flat terrain and low relative relief). On aerial photographs they exhibited dark tones and a smooth, fine, regular texture. The boundary with bedrock or surrounding deposits (especially with alluvial fans) was gradational and difficult to map with precision.

Debris deposits include colluvial and eluvial deposits, talus deposits and debris cones. Eluvial deposits were found on gentle slopes and on the tops of ridges. Colluvial deposits were particularly abundant where concavities were present in the slopes. Talus and debris cones were observed under rock cliffs. Talus locally formed an apron bounding the foot of the cliff, whereas debris cones were located at the outlets of steep channels. The characteristics of debris deposits on photographs varied widely. Eluvial sediments exhibited dark tones and fine texture; colluvial deposits showed dark to light tones and coarse to fine texture depending on the size, type and lithology of the debris. Talus and debris cones were distinguished by light tones and a coarse texture. Boundaries of the different types of debris were gradational, subdued and difficult to map.

An attempt was made to estimate the thickness of the debris cover. Thickness was tentatively ascertained with respect to the presence of concavities and convexities, local surface roughness and the mantling effect of debris on the underlying bedrock topography. Thick deposits concealed the form of the bedrock, in places completely, whereas thin covers of debris merely smoothed the underlying topography. As a rule of thumb, shallow deposits were assigned a thickness of no more than 4-5 m.

Bedrock

The bedrock class included areas where rocks of the Umbria-Marche stratigraphic sequence crop out or are covered by soil or a veneer of debris. The sequence extends from the Calcare Massiccio formation, which is Lias in age, to the Marnoso Arenacea formation, which is Miocene. Other classes of bedrock were Holocene deposits of travertine, and fluvial and lake deposits of Plio-Pleistocene age. Fluvial and lake sediments and travertine were mapped separately because the reconnaissance surveys carried out after the earthquakes revealed that damage to buildings and infrastructure in areas where these rocks crop out was particularly severe, especially where travertine was involved. This probably indicates seismic amplification due to lithological setting (for example, at Stravignano, Aggi and Pale).

DISCUSSION

As stated in the introduction, the goals of the project were to map the distribution of landslides and surface deposits; to study the type and pattern of fractures and landslides triggered by seismic shaking; and to investigate the relationships between the co-seismic ground effects and the distribution of pre-existing landslides and surface deposits.

The first goal was achieved by preparing the surface deposit and landslide inventory map. The map was the result of the systematic interpretation of aerial photographs of various scales, dates and types, and a reconnaissance survey conducted mainly along roads. Results of the interpretation exercise were merged with data obtained during both the reconnaissance investigations and specific field surveys designed to test the quality of the maps and solve local problems of interpretation.

The photo-geological map was compared with detailed 1:10,000 scale geological maps prepared by the Department of Earth Science at the University of Perugia. The comparison was performed on five map sheets covering about 200 km². It allowed us to assess the quality of the photo-geological map, which was found to be consistent and reliable. Mismatches between the geological and photo-geological maps were limited and mostly due to differing extents of shallow debris deposits, which were overestimated in the photo-geological map. The over-estimation was largely due to the difficulty of recognising the presence and extent of the debris deposits from aerial photographs. It should be noted that at the local scale deciding which map was correct was occasionally a matter of opinion. A field geologist who recognises a rock type and examines its structure at a few outcrops may map an area as bedrock, while a geomorphologist who uses aerial photographs to identify a veneer of detritus covering the bedrock may map the same area as a debris deposit.

The photo-geological map covers an area of about 900 km², of which 240 km² (26.7%) were mapped as surface deposits or landslides (tab. 1). Alluvial sediments (fig. 2a) covered about 67 km², while deposits in closed depressions (fig. 2b) covered 12 km²; and debris deposits (i.e., eluvial and colluvial cover, talus and debris cones - fig. 2c) covered about 128 km². Landslides (including debris flows) covered 33.3 km² (fig. 2d). At 3.7% of the study area this is lower than the percentage found in neighbouring areas where limestone crops out in steep terrain (for example, in the vicinity of Monte Coscerno, BARCHI *et alii*, 1993).

Deep-seated landslides ranged in size from a few hectares to more than a square kilometre. The largest failures were located where the Scaglia Bianca and Scaglia Rossa formations crop out (e.g., at Annifo, Franca, and Pian dell'Aia) and involved the underlying marl and clay of the Marne a Fucoidi formation. They were also found in the Bisciaro and the Scaglia Cinerea formations (e.g., at Liè). Deep-seated landslides were also found along major thrust faults (e.g., at Macchia and Sellano). The size and distribution of pre-existing, deep-seated failures was consistent with previous studies of the type and pattern of landslides in the Umbria-Marche Apennines (GUZZETTI *et alii*, 1996).

The type and pattern of ground effects triggered by seismic shaking were ascertained based on the informa-

TABLE 1

Surface deposits and landslide inventory map. Extent and percentage of the mapped classes.
- *Carta inventario dei movimenti franosi e dei depositi superficiali. Estensione e percentuali delle classi cartografate.*

	Area	
	km ²	%
Surface deposits	207.1	23.0
- Alluvial sediments	66.8	7.4
- Deposits in closed depressions	12.0	1.3
- Debris deposits	128.3	14.3
Thick (> 5 m)	53.8	6.0
Shallow (< 5 m)	74.5	8.3
Landslides (including debris flows)	33.3	3.7
Bedrock	659.6	3.7
Total	900.0	100

tion gathered during field surveys carried out after the major earthquakes. Ground effects observed in the field were mostly ground fractures and mass-movements. Compaction phenomena were observed mostly on embankments. Variations in the discharge and water quality of springs were reported near Nocera Umbra and Sellano. A few cases of surface faulting phenomena were also reported, mostly along pre-existing fault planes (CELLO *et alii*, 1998). The latter are not discussed in the paper.

Ground fractures were observed at 124 sites, for a total of 324 cracks ranging in length from less than 2 meters to more than 300 meters (fig. 3 and fig. 4). The majority of the cracks ranged in length from 10-100 meters, with an average value of about 40 meters. For most of the sites (63%) only one or two cracks were reported. Where more fractures were observed at the same site cracks were parallel, sub-parallel, perpendicular or arranged *en echelon*.

Reconnaissance field surveys revealed that most of the seismically induced ground fractures were related to the presence of anthropogenic features, such as embankments, roads, retaining walls and buildings. This was particularly clear along roads built by cut and fill methods (fig. 4). Fractures from a few metres to some tens of metres long opened in the middle of roads or in sections built on fill, and were either parallel or perpendicular to the road. In places, fractures opened where roads were built on debris or landslide deposits.

Most of the fractures were located along the slopes (about 70%), and only a minority were observed in flat terrain, on valley floors or on ridge tops. Ground fractures were mostly open, from a few millimetres to some centimetres, but only a few (less than 10%) exhibited a distinct vertical displacement. Of about 320 mapped fractures, 52% were located within a distance of 4 km, and about 90% were within 23 km from the epicentral area, defined as the line joining the epicentres of the 26 September and 14 October earthquakes.

Landslides triggered by seismic shaking were chiefly rockfalls (fig. 5), minor rockslides (fig. 6) and rock topples (fig. 7). This agrees with what is expected from the

energy released by earthquakes of $M_L < 6.0$ (KEEFER, 1984). The distribution of rockfalls fitted the observed macroseismic intensity pattern. We mapped a total of 253 mass-movements at 104 sites. In most of the sites (64%) only one or two failures were reported. In 31% of the sites 3 to 5 failures were observed, and in 5% of the sites more than 5 failures were observed. Rockfalls, minor rockslides and rock topples accounted for 93% of the reported mass-movements. The other landslides were equally distributed between debris falls or debris slides, and complex slides. These figures differ partially from those reported by BOZZANO *et alii* (1998) and by ESPOSITO *et alii* (2000). The differences refer mostly to translational, rotational and complex landslides that were not recognised by us. Along roads we observed compaction phenomena that locally could have been classified as rotational or complex landslides.

The number of rockfalls at each site may have been larger than reported, particularly where failures were abundant (i.e., in places along the Nera valley, and near Sellano – fig. 5) or they were very small (less than 0.001 m^3). Many rockfalls occurred along road escarpments. About 50% of all reported rockfalls for which the information is available were triggered from escarpments less than 10 meters high. The remaining 50% occurred from higher escarpments, up to hundreds of meters high. Rockfalls ranged in size from a cubic decimetre to few tens of cubic meters, depending on the type and quality of the rock.

The distribution of rockfalls (including topples and minor rockslides) fitted the observed macroseismic intensity pattern (fig. 3). Of the 65 rockfall sites for which the date of occurrence of the event is known, 33 sites were visited before the 14 October earthquake (i.e., they were triggered by the September 26 earthquakes or by some of the strongest aftershocks), and 32 sites were visited after the 14 October earthquake (fig. 8).

Fig. 9 shows the distance of the rockfalls from the earthquake epicentres. Failures triggered by the 26 September earthquakes (and the subsequent aftershocks – squares in fig. 9) occurred mostly within a distance of 8 km from the epicentre, and were observed at a maximum distance of 15 km from the epicentre (fig. 8). Failures triggered by the 14 October earthquake (triangles in fig. 9) exhibited a similar behaviour; they occurred mostly within 8 km from the epicentre and were reported at a maximum distance of 19 km from the epicentre (fig. 8). Fig. 9 also shows a curve (open diamonds) for all reported rockfalls (including topples and minor rockslides), regardless of the date of occurrence. The data-set includes also rockfalls for which the date of occurrence is unknown or that were triggered weeks after the 14 October earthquake. The «cumulative» data-set shows that about 50% of all reported failures occurred within 8 km from the epicentral area, defined as the line joining the 26 September and the 14 October earthquakes. The maximum observed distance for the «cumulative» data-set is 25 km. These values are in agreement with the figures proposed by ESPOSITO *et alii* (2000), even if the spatial distribution of mass-movements is locally different.

The earthquakes of 26 September triggered rockfalls, topples and small rockslides ranging in size from a few cubic decimetres to a few tens of cubic metres (for example, at Pale and Bagni di Stravignano – fig. 7). Some of the largest aftershocks also caused such mass movements

(e.g., at Bagni di Stravignano). The earthquake of 14 October triggered tens of failures, mostly to the South and to the East of the epicentre (fig. 8). Rockfalls and rockslides were particularly abundant near Triponzo, where they threatened a high voltage power line; along the Corno river, where artificial tunnels and defensive elastic fences were destroyed and state road no. 320 was damaged; between Piedipaterno and Triponzo, where elastic fences were destroyed and state road no. 209 was damaged; and along the Vigi Valley near Sellano, where the access road to a dam was blocked and a water channel was damaged (fig. 5).

Rockfalls were also triggered by relatively low-magnitude aftershocks. This was the case of a rockslide-rockfall along the Fonno Valley near La Rocchetta to the East of Gualdo Tadino. At 10:30 p.m. on 7 November 1997 $50\text{--}100 \text{ m}^3$ of Calcare Massiccio limestone detached from a sharp ridge at an elevation of about 850 m, fell 30–50 metres down the talus slope, and broke into several pieces that proceeded to roll and bounce downhill until they reached a road, where one of the rock fragments destroyed a car. Another example is given by the rockfall that in the early afternoon of 4 April 1998 fell on state road no. 77, near Pale. Apparently, these rockfalls were not triggered by intense aftershocks. Most probably the failures were induced by the cumulative effect of repeated ground shaking. The influence of ground shaking on unstable rocks was particularly apparent at Stravignano southeast of Nocera Umbra, where a 10m-thick travertine cap was fractured by the earthquakes of 26 September 1997 was then subject to repeated, but minor, rock falls (for example on 3 October at 10:56 a.m.), and finally collapsed during the night of 16–17 October 1997. The travertine cap failed along a large, pre-existing fracture and formed large topples that fell onto the adjacent road.

A few co-seismic ground fractures were mapped in or near deep-seated landslide deposits. Fractures were mostly rectilinear, from a few millimetres to about a centimetre wide, and either single or multiple. In a few places, the downslope rim dropped a few decimetres (e.g., in the Monte Annifo landslide, fig. 10c) suggesting a mass movement, but no major landslide was reactivated to the point of catastrophic failure. Mapping of the co-seismic fractures and of the pre-existing landslides showed that many fractures were located at the boundary between the landslide deposit and the stable ground, which was usually bedrock. Ground fractures occurred along the side of a landslide (for example SE of Franca – see fig. 10a), near the crown area (e.g., at Afrile), or inside a landslide deposit (e.g. Franca – see fig. 10a or Annifo – see fig. 10b). This suggests that fractures were produced by differential shaking between the landslide deposit and its surrounds, and not by the downslope movement of a landslide.

The case of the Pian dell'Aia landslide (fig. 10c) was different. Due to its remote position north of Nocera Umbra, the area was first visited only on 10 October 1997. It was identified as a deep-seated, complex landslide and fractures were observed on its southern side. A second survey carried out in May 1998 revealed that the fractures had enlarged and a distinct graben had cut into previously stable ground. The seismically-induced fractures were limited to a small portion of the landslide crown but were clearly enlarged with respect to the pre-existing landslide scarp. No deformation was observed further downslope.

Due to the small number of complex landslides triggered (or involved) by seismic shaking, a detailed investigation of the relationship between landslide position and its distance to the epicentre is not significant. We observe that the larger distance of an earthquake induced landslide (the Pian dell'Aia landslide) from the epicentral area is 24 km.

CONCLUSION

The earthquake sequence that began in September 1997 in the Umbria-Marche Apennines triggered landslides and opened up ground fractures. Landslides were mostly rockfalls, rock topples and minor rockslides. Failures were triggered by the most intense earthquakes and by some of the aftershocks. The cause of some of the failures was the cumulative effect of ground shaking produced by numerous aftershocks. Co-seismic ground fractures were mostly related to the presence of anthropogenic structures, such as embankments, roads, retaining walls and buildings. Failures along sections of road built on fill were particularly abundant.

To study the distribution of ground effects due to seismic shaking we drew up a surface deposits and landslide inventory map. This was prepared through the systematic analysis of aerial photographs, and field surveys. Since large scale geological maps cover only a small fraction of the territory, the map represents a first attempt to distinguish surface deposits including landslides from bedrock in the study area. The distinction is important as the pattern of damage due to seismic shaking was clearly influenced by the presence of travertine, pre-existing landslide deposits, and debris deposits. Of the entire study area, more than 25% was found covered by landslides or surface deposits. This is an important part of the territory, often neglected by the geological mapping. The map may prove useful for planning purposes and to help determine seismic hazards. Seismic amplification can be determined for landslides, for surface deposits, and at the boundary between surface deposits and the bedrock. These settings are well known to be prone to seismic amplification.

ACKNOWLEDGEMENT

We are grateful to several volunteer geologists who worked with us in the weeks after the earthquakes to collect valuable information on co-seismic fractures and landslides. We acknowledge the support of the Department of Civil Protection, and particularly of Cesare Landrini, who provided logistical support and aerial photographs. We thank David Alexander for reviewing the manuscript. Comments of the referees, David Keefer and Janusz Wasowski, improved the paper. The research was financed by grants from CNR-IRPI and CNR-GNDICI. The paper is GNDICI publication n. 2229.

REFERENCES

- ALLUM J.A.E. (1966) - *Photogeology and regional mapping*. Institute of Geological Sciences, Photogeological Unit, Pergamon Press, Oxford, pp. 107.
- AMADESI E. (1977) - *Manuale di fotointerpretazione con elementi di fotogrammetria*. Pitagora Editrice, Bologna, pp. 182 (in Italian).
- ANTONINI G., CARDINALI M., GUZZETTI F., REICHENBACH P. & SORRENTINO A. (1993) - *Carta Inventario dei Fenomeni Franosi della Regione Marche ed aree limitrofe*. CNR-GNDICI publication no 580, 2 map sheets, 1:100,000 scale (in Italian).
- BARCHI M., CARDINALI M., GUZZETTI F. & LEMMI M. (1993) - *Relazioni fra movimenti di versante e fenomeni tettonici nell'area del M. Coscerno-M. di Civitella, Val Nerina (Umbria)*. Boll. Soc. Geol. It., **112**, 83-111 (in Italian).
- BOSCHI E., GUIDOBONI E., FERRARI G. & VALENSISE G. (1998) - *I Terremoti dell'Appennino Umbro-Marchigiano. Area sud orientale dal 99 a.C. al 1984*. ING and SGS Storia Geofisica Ambiente, Topografia Compositori Pub., Bologna, 267 pp. (in Italian).
- BOZZANO F., GAMBINO P., PRESTININZI A., SCARASCIA MUGNOZZA G. & VALENTINI G. (1998) - *Ground effects induced by the Umbria-Marche earthquakes of September-October 1997, Central Italy*. 8th International IAEG Congress, Balkema, Rotterdam, 825-830.
- CELLO G., DEIANA G., MANGAMO P., MAZZOLI S., TONDI E., FERRELLI L., MASCHIO L., MICHETTI A.M., SERVA L. & VITTORI E. (1998) - *Evidence of surface faulting during the September 26 Colfiorito (Central Italy) earthquakes*. J. Earthquake Eng., **2**, 303-342.
- ESPOSITO E., PORFIDO S., SIMONELLI A.L., MASTROLORENZO G. & IACCARINO G. (2000) - *Landslides and other surface effects induced by the 1997 Umbria-Marche seismic sequence*. Engineering Geology, **58**, 353-376.
- GUZZETTI F. & CARDINALI M. (1989) - *Carta Inventario dei Fenomeni Franosi della Regione dell'Umbria ed aree limitrofe*. CNR-GNDICI publication no. 204. 2 map sheets, 1:100,000 scale (in Italian).
- GUZZETTI F., CARDINALI M. & REICHENBACH P. (1996) - *The influence of structural setting on lithology on landslide type and pattern*. Environmental and Engineering Geoscience, **2** (4), Winter 1996, 531-555.
- KEEFER D.K. (1984) - *Landslide caused by earthquakes*. Geological Society of America Bulletin, **95**, 406-421.
- MILLER V.C. (1961) - *Photogeology*. McGraw Hill Book Company, New York, pp. 248.
- RAY R.G. (1960) - *Aerial photograph in geologic interpretation and mapping*. U.S. Geological Survey Professional Paper 373, Washington, pp. 230.
- RIB H.T. & LIANG T. (1978) - *Recognition and Identification*. Chapter 3. In: Schuster R.L. & and Krizek R.J. (eds.), Landslides Analysis and Control, Transportation Research Board, Washington, D.C. 1978, 34-80.
- SERVIZIO SISMICO NAZIONALE & ENEL (1998) - *Elaborazioni delle principali registrazioni accelerometriche della sequenza sismica umbro-marchigiana del settembre ottobre 1997*. Servizio Sismico Nazionale, Rome, May 1998, 3 volumes and a Cd-Rom (in Italian).
- SGA, STORIA GEOFISICA AMBIENTE (2000) - *Fenomeni franosi in Italia indotti da terremoti (secc. XIII-XX)*. CNR Research contract 99.00152-42, Unpublished report, pp. 137 (in Italian).
- VAN ZUIDAN R.A. (1985) - *Aerial Photo-Interpretation in Terrain Analysis and Geomorphologic Mapping*. International Institute for Aerospace Survey and Earth Sciences, Smits Publishers, The Hague, pp. 442.